Mathematical Modeling in Natural Extract Anti-Reflection Coatings using Green Synthesis Method

Snehal Marathe
Sinhgad College of Engineering, Army Institute of Technology, Pune, India
snehalmarathe@gmail.com (corresponding author)

B. P. Patil
Army Institute of Technology, Pune, India
Bp_patil@rediffmil.com

Shobha Waghmode
MES Abasaheb Garware College, Pune, India
shobhawaghmode@gmail.com

Received: 17 April 2024 | Revised: 9 May 2024 | Accepted: 12 May 2024

 DOI: https://doi.org/10.48084/etasr.7525

ABSTRACT

The use of renewable energy sources to replace conventional energy sources like fossil fuels is essential. Solar panels are the most widespread technology for clear energy production. However, is crucial to raise the efficiency of solar panels. A large portion of sunlight is reflected by the front surface of the panel and thus the use of an Anti-Reflecting Coating (ARC) has become significant in raising the efficiency of solar panels, through reducing the reflection losses. The ARCs made of natural extracts were utilized to improve the efficiency of Silicon solar panels. The natural extracts were produced from Kailashpati fruit juice and Badminton ball tree flower powder. In the synthesis of these natural extracts, monometallic gallium chloride nanoparticles were used to check their effect on the efficiency of solar power generation. The novelty of this paper is the attempt to mathematically calculate the absorbance of the ARCs, at a particular wavelength, with the use of the refractive indices and thicknesses of ideal ARCs.

Keywords-ARC; solar panel; power generation; natural extract materials; green synthesis method

I. INTRODUCTION

Since most of the sunlight that strikes a solar panel is reflected, the use of Anti-Reflective coatings (ARCs) has become more and more important in increasing solar panel efficiency [1]. The ARC is mainly applied to glass substrates, but in certain scenarios, it is also applied to polymer substrates [2]. The polymer substrates have low heat resistance; hence, they have low adhesion and optical transmittance capacity [3]. To provide superior passivation qualities and lower reflection, solar cells are processed using ARCs [4]. This causes the generated current to significantly rise, which increases the efficiency of the cell [5].

Thin films, either single or multilayers, are typically used to create modern ARCs [6]. For all the incidence angles throughout a broad solar spectrum, the optimal ARC structure should result in 0% reflection loss on the surfaces of solar cells [7]. It is commonly known that a single layer ARC needs to have a specific Refractive Index (RI) and can reduce normal-incidence reflection at limited wavelengths and usually are around 600 nm [8, 9].

The availability of materials with the necessary RIs limits the use of single-layer thin-film ARC [10]. However, it is also recognized that a single-layer ARC cannot cover a large portion of the solar spectrum [11], hence the use of a double-layer ARC is being explored [12]. However, several requirements must be met for the thicknesses and RIs of the top and bottom layers of the double layer ARC [13].

The ARC's efficiency is determined by two factors: the material RI and film thickness. Variations in RI are responsible for optical reflection [14]. ARCs made from nanomaterials such as TiO_2, SiO_2, MgF_2 and others have been used [15]. Many techniques are used for synthesizing titanium oxide and gallium chloride nanoparticles. Different sizes and forms of nanoparticles have been created using a variety of chemical and physical techniques. However, these processes require several steps, a lot of energy, challenging purification, and the use of hazardous chemicals. Green synthesis techniques, which use

plant extracts or biological microbes, have therefore become a straightforward substitute for classical chemical synthesis. It is inexpensive, safe for the environment, and simple to scale up for large-scale synthesis. The green synthesis of nanomaterials for ARCs is advantageous due to its simplicity, environmental friendliness, and lower cost.

Various wide bandgap materials are used as ARC materials for reducing the reflection losses in the various generations of solar cells. Some of the popular materials that are used as ARC are SiO_2, TiO_2, Al_2O_3, SiO_2-TiO_2, ZnO, ZnO-TiO_2, ZnS, MgF_2, etc., but these materials reduced the reflection losses to a certain extent, and the overall Power Conversion Efficiency (PCE) of solar cells was only improved slightly. Therefore, a suitable material is required to improve the electrical, optical, transmittance, reflectivity, and PCE of the solar cells. A new hybrid system for increasing the efficiency of solar panels using monometallic gallium chloride (GC) ARCs is designed. The absorbances of the combination of monometallic coatings with ionic and poly-ionic liquids as ARCs are verified using mathematical modeling. Absorption, efficiency, electrical conductivity, transparency, and wettability (i.e., hydrophobicity or hydrophilicity) are important characteristics of the coatings that are meant to optimize performance. There are several methods for coating surfaces, including diffusion coatings, chemical and physical vapor deposition, thermal spraying, electro deposition, electro less deposition, and laser-based processes.

II. EXPERIMENTAL AND METHODS

A. Characteristics of ARC

A good ARC should have the following characteristics:

- The materials' characteristics need to remain unchanged while humidity levels fluctuate.
- Withstand temperature levels, atmospheric corrosion, and oxidation.
- Should be stable in vacuum and air.
- The stability of the coating's optical and physical qualities is crucial.
- It is necessary for the coating to have strong adhesion to the substrate.
- The ARC should be reasonably priced.

B. Anti-Reflecting Coating Gallium Chloride using Green Synthesis Method

Green synthesis techniques, which use plant extracts or bacteria, have become a popular and straightforward substitute for classical chemical synthesis. Green synthesis is superior to other chemical approaches because it is less expensive, more environmentally friendly, and easier to scale up for large-scale synthesis. Because it avoids the complex process of maintaining cell cultures and may be appropriately scaled up for large-scale manufacturing in non-aseptic settings, the synthesis of nanoparticles using plant extracts can be beneficial over other biological procedures [16]. The green synthesis of different natural extracts for the preparation of monometallic nanoparticles is preferred. The different natural extracts used in this work were derived from the Kailashpati fruit and Badminton ball tree flower powder. The preparation of the extracts is presented in Figure 1, and the synthesis of gallium chloride nanoparticles is presented in Figure 2.

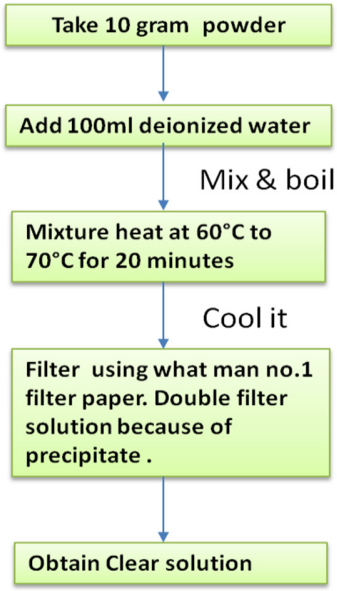

Fig. 1. Preparation of extract.

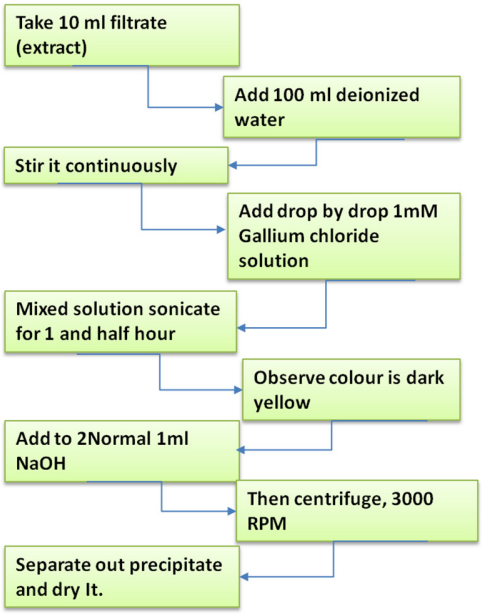

Fig. 2. Synthesis of gallium chloride nanoparticles.

C. Preparation of Gallium Chloride Solution

Details for the preparation of the gallium chloride solution can be found in our previous work [17]. Briefly, to 1 L of deionized water is added 0.352 g $GaCl_3$ to make a 2 Mm solution. The solution was shaken and then sonicated for 10 minutes at room temperature.

III. MATHEMATICAL MODELING

A modified transfer matrix approach is applied for each configuration to determine the reflectance from the silicon surface. Calculating the average reflectivity is crucial since the sun spectrum spans a wide wavelength range, from 400 to 1100 nm. We define the average residual reflection factor, R_m, as follows:

$$R_m = \frac{1}{\lambda_{max}-\lambda_{min}} \int_{\lambda_{min}}^{\lambda_{max}} R(\lambda) d\lambda \quad (1)$$

Where, λ_{max} and λ_{min} are the wavelength range's maximum and lowest values, respectively. The reflection factor is denoted as $R(\lambda)$. Taking into consideration the AM 1.5 solar spectrum is crucial when comparing the efficacy of an ARC on a solar cell. The 400 nm to 1100 nm wavelength region of the sun spectrum has been selected for our inquiry, because photons with wavelengths longer than 1100 nm are not absorbed by silicon and photons with wavelengths lower than 400 nm have nearly negligible spectral power density in the AM 1.5 spectrum.

The transmission matrices of the ARC layers may be used to compute the reflection $R(\lambda)$. That relies on both the refractive index $n(\lambda)$and extinction coefficient $k(\lambda)$. A transfer matrix approach is utilized to determine the silicon surface reflectance for each configuration. The ARC structures represented in Figure 3 can be considered to be composed of two layers. Therefore, three interfaces are formed on a Si substrate.

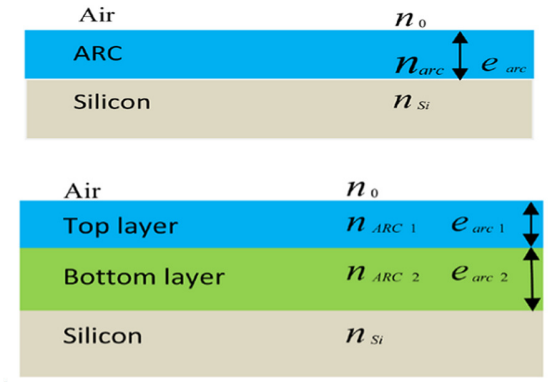

Fig. 3. (a) Single-layer antireflection coating-equipped silicon solar cell structure and (b) double-stack antireflection coating-equipped silicon solar cell structure.

First, below is explained a single layer's characteristic matrix. The matrix that defines the single antireflection layer issue has the following relationship:

$$\begin{bmatrix} E_0 \\ H_0 \end{bmatrix} = M \begin{bmatrix} E(S_i) \\ H(S_i) \end{bmatrix} \quad (2)$$

M is a matrix given by:

$$M = \begin{bmatrix} cos\,\psi & \frac{i\,sin\,\psi}{\eta_{arc}} \\ i\,sin\,\psi \times \eta_{arc} & cos\,\psi \end{bmatrix} \quad (3)$$

A multilayer's characteristic matrix is the result of multiplying matching single layer matrices. It becomes the following for a double layer antireflection coating:

$$\begin{bmatrix} E_0 \\ H_0 \end{bmatrix} = M_1 M_2 \begin{bmatrix} E(S_i) \\ H(S_i) \end{bmatrix} = M_t \begin{bmatrix} E(S_i) \\ H(S_i) \end{bmatrix} \quad (4)$$

The M_t is given by:

$$M_t = \begin{bmatrix} \cos\psi & \frac{i\sin\psi_1}{\eta_{arc1}} \\ i\sin\psi \times \eta_{arc1} & \cos\psi_1 \end{bmatrix} \times \begin{bmatrix} \cos\psi & \frac{i\sin\psi_2}{\eta_{arc2}} \\ i\sin\psi \times \eta_{arc2} & \cos\psi_2 \end{bmatrix} \quad (5)$$

where $i^2 = -1$ and η_{arc1}, η_{arc2} indicate the top and bottom antireflection layers' respective refractive indices [18], which were measured using the RSR – 2, Rajdhani ABBE Refractometer. ψ_1 and ψ_2 are dephasing among the reflected waves of layers k and k+1, respectively.

$$\psi_1 = \frac{2\pi}{\lambda}\eta_{arc1}e_{arc1}, \psi_2 = \frac{2\pi}{\lambda}\eta_{arc2}e_{arc2} \quad (6)$$

The detailed derivation of amplitude reflection (r) and transmission coefficients (t) are given below:

$$r = \frac{n_0 M_{11} + n_0 n_{si} M_{12} + M_{21} - n_{si} M_{22}}{n_0 M_{11} + n_0 n_{si} M_{12} + M_{21} + n_{si} M_{22}} \quad (7)$$

where M_{ij} are the components of the multilayer's characteristic matrix. The reflectivity and absorptance coefficients are as follows:

$$R = |r|^2 \quad (8)$$

$$A = 1 - R \quad (9)$$

where n_{si} and n_0 are the silicon and vacuum's respective refractive indices.

IV. RESULTS

A. Synthesis of Monometallic Nanoparticles Using Kailashpati Fruit Extracts (GK)

One fresh Kailashpati fruit was washed and dried properly. Later, it was cut into small pieces to make a fine paste. This fine paste, i.e., the fruit juice, was mixed in 500 ml of deionized water. The mixture was then boiled for 20 minutes at 70 to 80°C and then cooled down. The solution was then filtered using Whataman No. 1 filter paper. The prepared clear filtrate was further used for synthesis. Gallium chloride (2 Mm) metal salt was dissolved in 1000 ml of deionized water. Ten flasks were taken and a 100-ml mixture of gallium chloride and deionized water to each flask was added. Also, 4 ml of Kailashpati fruit extract were added to each flask, and then the solution was sonicated for 60 minutes to maintain its pH. After 24 hours, the nanoparticles settled down and the color changed. The nanoparticles were further centrifuged at 3000 RPM and then separated. The separated nanoparticles were dried to 40–50 °C, and the powder was characterized with Scanning Electron Microscopy (SEM). Figure 4 shows the SEM image of the particles, from which a particle size of 80 nm was estimated. Figure 5 illustrates the UV absorption spectrum of GK produced via green synthesis. The solution extract was sprayed over the solar panel with a spray bottle.

B. Calculations for GK

From (6) using the values λ = 260 nm, η_{arc} = 1.361, e_{arc} = 80 nm we get: ψ=2.629, cosψ=0.998, and sinψ=0.045. Then according to (3) the M is:

$$M = \begin{bmatrix} 0.998 & 0.033i \\ 0.061i & 0.998 \end{bmatrix} = \begin{bmatrix} M_{11} & M_{12} \\ M_{21} & M_{22} \end{bmatrix}$$

Using the values n_0=1.003 and n_{si}=3.929 in (7) we get:

$$r = 0.061i - 0.591$$

and then from (8) we calculate R = 0.346 and from (9):

A=0.654

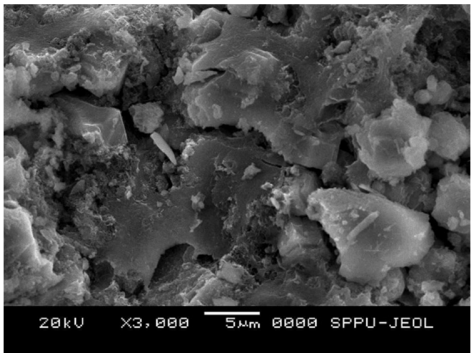

Fig. 4. SEM image of GK.

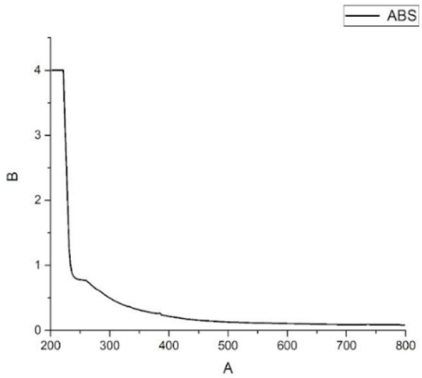

Fig. 5. UV absorption spectrum of GK via green synthesis.

C. Synthesis of Monometallic Nanoparticles Using Flower Badminton Ball Tree Extract (GF)

The Badminton ball tree has the botanical name Parkia biglandulosa, from which the dry flower powder was produced. The dry flower powder was mixed with 70 ml deionized water in a beaker. This mixture was then boiled at 80 to 90°C for 20 minutes. After cooling the solution was then filtered using Whatman no.1 filter paper. This clear filtrate was used for further synthesis of nanomaterials. Gallium flower powder coating: gallium chloride (2 Mm) metal salt was dissolved in 1000 ml of deionized water. Take 10 flasks and add a 100-ml mixture of gallium chloride and deionized water to each flask. Add 4 ml of flower extract to each flask, and then sonicate the solution for 60 minutes to maintain its pH. After 24 hours, these nanoparticles settle down and the color changes. The nanoparticles were further centrifuged at 3000 RPM and then separated. The separated nanoparticles were dried at room temperature (40–50 °C), and the powder was characterized. The UV absorption spectrum of GF produced via green synthesis is presented in Figure 6.

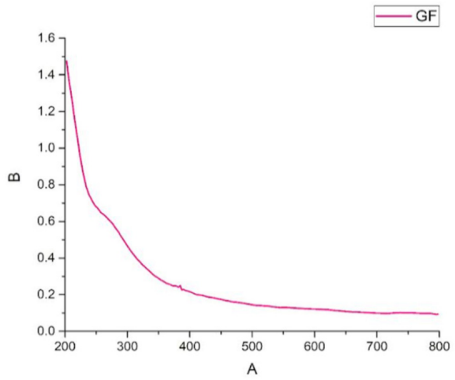

Fig. 6. UV absorption spectrum of GF via green synthesis.

D. Calculation for GF

Similar as before, from (6) using the values λ = 260 nm, η_{arc} = 1.351, e_{arc} = 80 nm we get: ψ=2.611 and cosψ=0.999, sinψ=0.046. Then according to (3) the M is:

$$M = \begin{bmatrix} 0.999 & 0.034i \\ 0.062i & 0.999 \end{bmatrix} = \begin{bmatrix} M_{11} & M_{12} \\ M_{21} & M_{22} \end{bmatrix}$$

Using the values n_0=1.003 and n_{si}=3.929 in (7) and (8) we get:

R=0.354 and from (9):

A=0.646

Table I shows the theoretical and experimental values of absorbance for the GK and GF.

TABLE I. THE THEORETICAL AND EXPERIMENTAL VALUES OF ABSORBANCE, A, IN DIFFERENT COATINGS

Coating	A, theoretical	A, experimental
GK	0.654	0.7
GF	0.646	0.642

E. Efficiency and Power of Coated and Uncoated Panels

The results of the coated and uncoated Si solar panels have been published in our previous work [17]. The experimental set up was described in [17]. Briefly, five devices were designed to measure the voltage and current across the load connected with the solar panels. In one device the lux meter was mounted to measure the sun intensity. One panel was kept uncoated, and the others were coated with the proposed ARCs. The parameters measured for uncoated and coated panels were the voltage, current, power output, and temperature of the panel.

The power output of the solar panel was measured across the load which had three 100-ohm resistors connected in parallel. The resistance was 33.3 Ohm for each panel. The sensor used for current, and voltage was the Power Chip named INA226. Main IOT chip was ESP8266 – processor + wifi module, SOC. A common light sensor using a large LDR was calibrated against a light meter. A lux meter was used to calibrate the LDR unit. The Grafana software was used to directly download the excel sheets for the voltage, current, power output and temperature of the coated and uncoated panels.

The efficiency and the maximum power generated, Pmax, of the panels along with other photovoltaic parameters are listed below in Table II. The area of solar panel was 20.5 cm x 30 cm. The solar irradiance was assumed constant at 1000 W/m^2. The efficiency was calculated by dividing the Pmax with the solar panel area and the solar irradiance. The total annual hours of available sun in Pune, India was assumed 2870 h.

TABLE II. OUTPUT OF THE SOLAR PANELS

	Uncoated	**GT**	**GK**
Pmax (W)	7.2	9.11	8.8
Efficiency (%)	11.7	14.8	14.3
Energy generated for 1 h (Wh)	45	57.4	55
Annual energy generated (kWh)	129.15	164.82	157.85

The increase in power output when compared with uncoated panels was 27.61% for GT-coated panels, 22.77% for GF-coated panels, and 22.59% for the GK-coated panels. The improvement in efficiency highlights the positive impact of ARC on enhancing the energy production of solar panel systems.

V. CONCLUSIONS

From mathematical calculations, the absorbance was verified theoretically and practically for the GF and GK anti-reflecting coatings. Also, coated panels gave an average 1.5-watt power output more than uncoated panels. The results reported in this study can be used as an important tool for improving the efficiency of existing solar panels. However, for an ideal antireflection layer, the absorption loss, especially in the wavelength range [400–1100 nm], must be low. The decrease in absorbance of light with a random planar front surface is observed due to the absence of light scattering by the ARC. More wide and thorough investigation is required since the findings and results could assist further studies to discover the most ideal materials that can be used as an ARC and will enhance the efficiency of silicon solar cells more significantly. To advance the evaluation and improvement for industrial purposes, the scheme should be developed as a real model.

REFERENCES

[1] A. Afzal, A. Habib, I. Ulhasan, M. Shahid, and A. Rehman, "Antireflective Self-Cleaning TiO_2 Coatings for Solar Energy Harvesting Applications," *Frontiers in Materials*, vol. 8, Jun. 2021, Art. no. 687059, https://doi.org/10.3389/fmats.2021.687059.

[2] G. Hashmi, M. J. Rashid, Z. H. Mahmood, M. Hoq, and Md. H. Rahman, "Investigation of the impact of different ARC layers using PC1D simulation: application to crystalline silicon solar cells," *Journal of Theoretical and Applied Physics*, vol. 12, no. 4, pp. 327–334, Dec. 2018, https://doi.org/10.1007/s40094-018-0313-0.

[3] A. V. Deinega, I. V. Konistyapina, M. V. Bogdanova, I. A. Valuev, Yu. E. Lozovik, and B. V. Potapkin, "Optimization of an anti-reflective layer of solar panels based on ab initio calculations," *Russian Physics Journal*, vol. 52, no. 11, pp. 1128–1134, Nov. 2009, https://doi.org/10.1007/s11182-010-9350-0.

[4] G. Rajan, S. Karki, R. W. Collins, N. J. Podraza, and S. Marsillac, "Real-Time Optimization of Anti-Reflective Coatings for CIGS Solar Cells," *Materials*, vol. 13, no. 19, Sep. 2020, Art. no. 4259, https://doi.org/10.3390/ma13194259.

[5] U. Sikder and M. A. Zaman, "Optimization of multilayer antireflection coating for photovoltaic applications," *Optics & Laser Technology*, vol. 79, pp. 88–94, May 2016, https://doi.org/10.1016/j.optlastec.2015.11.011.

[6] J. Hossain, B. K. Mondal, S. K. Mostaque, S. R. A. Ahmed, and H. Shirai, "Optimization of multilayer anti-reflection coatings for efficient light management of PEDOT:PSS/c-Si heterojunction solar cells," *Materials Research Express*, vol. 7, no. 1, Dec. 2019, Art. no. 015502, https://doi.org/10.1088/2053-1591/ab5ac7.

[7] O. Pawar, N. Deshpande, S. Dagade, S. Waghmode, and P. Nigam Joshi, "Green synthesis of silver nanoparticles from purple acid phosphatase apoenzyme isolated from a new source Limonia acidissima," *Journal of Experimental Nanoscience*, vol. 11, no. 1, pp. 28–37, Jan. 2016, https://doi.org/10.1080/17458080.2015.1025300.

[8] H. Abdullah, A. Lennie, and I. Ahmad, "Modelling and Simulation Single Layer Anti-Reflective Coating of ZnO and ZnS for Silicon Solar Cells Using Silvaco Software," *Journal of Applied Sciences*, vol. 9, no. 6, pp. 1180–1184, 2009, https://doi.org/10.3923/jas.2009.1180.1184.

[9] A. Bahrami, S. Mohammadnejad, N. J. Abkenar, and S. Soleimaninezhad, "Optimized Single and Double Layer Antireflection Coatings for GaAs Solar Cells," *International Journal of Renewable Energy Research (IJRER)*, vol. 3, no. 1, pp. 79–83, Mar. 2013.

[10] N. Shanmugam, R. Pugazhendhi, R. Madurai Elavarasan, P. Kasiviswanathan, and N. Das, "Anti-Reflective Coating Materials: A Holistic Review from PV Perspective," *Energies*, vol. 13, no. 10, Jan. 2020, Art. no. 2631, https://doi.org/10.3390/en13102631.

[11] M. Moayedfar and M. K. Assadi, "Various Types of Anti-Reflective Coatings (Arcs) Based on the Layer Composition and Surface Topography: A Review," *Reviews on Advanced Materials Science*, vol. 53, no. 2, pp. 187–205, Feb. 2018, https://doi.org/10.1515/rams-2018-0013.

[12] H. Kanda *et al.*, "Al_2O_3/TiO_2 double layer anti-reflection coating film for crystalline silicon solar cells formed by spray pyrolysis," *Energy Science & Engineering*, vol. 4, no. 4, pp. 269–276, 2016, https://doi.org/10.1002/ese3.123.

[13] M. Subramanian *et al.*, "Optimization of Antireflection Coating Design Using PC1D Simulation for c – Si Solar Cell Application," *Electronics*, vol. 10, no. 24, Jan. 2021, Art. no. 3132, https://doi.org/10.3390/electronics10243132.

[14] Y. F. Makableh, H. Alzubi, and G. Tashtoush, "Design and Optimization of the Antireflective Coating Properties of Silicon Solar Cells by Using Response Surface Methodology," *Coatings*, vol. 11, no. 6, Jun. 2021, Art. no. 721, https://doi.org/10.3390/coatings11060721.

[15] A. Diaw *et al.*, "Optimization of Antireflective Layers of Silicon Solar Cells: Comparative Studies of the Efficiency Between Single and Double Layer at the Reference Wavelength," *American Journal of Physics and Applications*, vol. 9, no. 6, pp. 133–138, Nov. 2021, https://doi.org/10.11648/j.ajpa.20210906.11.

[16] S. Waghmode, P. Chavan, V. Kalyankar, and S. Dagade, "Synthesis of Silver Nanoparticles Using *Triticum aestivum* and Its Effect on Peroxide Catalytic Activity and Toxicology," *Journal of Chemistry*, vol. 2013, Jun. 2013, Art. no. 265864, https://doi.org/10.1155/2013/265864.

[17] S. A. Marathe, B. P. Patil, S. A. Waghmode, and T. S. Zaware, "Analyses of Monometallic Nano Particle Coatings to Increase Solar Panel Efficiency," *Tuijin Jishu/Journal of Propulsion Technology*, vol. 44, no. 6, pp. 2516–2536, Dec. 2023.

[18] M. M. Diop *et al.*, "Optimization and Modeling of Antireflective Layers for Silicon Solar Cells: In Search of Optimal Materials," *Materials Sciences and Applications*, vol. 9, no. 8, pp. 705–722, Jul. 2018, https://doi.org/10.4236/msa.2018.98051.